HHS Public Access

Author manuscript

Mol Cancer Ther. Author manuscript; available in PMC 2018 January 01.

Published in final edited form as:

Mol Cancer Ther. 2017 January ; 16(1): 143–155. doi:10.1158/1535-7163.MCT-16-0413.

MENA confers resistance to paclitaxel in triple-negative breast cancer

Madeleine J. Oudin[1], **Lucie Barbier**[1,2], **Claudia Schäfer**[1], **Tatsiana Kosciuk**[1], **Miles A. Miller**[3,4], **Sangyoon Han**[5], **Oliver Jonas**[1], **Douglas A. Lauffenburger**[1,3], and **Frank B. Gertler**[1,6]

[1]David H. Koch Institute for Integrative Cancer Research, Massachusetts Institute of Technology, Cambridge, MA, USA

[2]ENS-Cachan, 61 avenue du President Wilson, 94235, Cachan, France

[3]Department of Biological Engineering, Massachusetts Institute of Technology, Cambridge, MA, 02139, USA

[4]Center for Systems Biology, Massachusetts General Hospital and Harvard Medical School, Boston, MA 02114

[5]Lydia Hill Department for Bioinformatics, UT Southwestern Medical Center, Dallas, TX, USA

[6]Department of Biology, Massachusetts Institute of Technology, Cambridge, MA, 02139, USA

Abstract

Taxane therapy remains the standard of care for triple-negative breast cancer. However, high frequencies of recurrence and progression in treated patients indicate that metastatic breast cancer cells can acquire resistance to this drug. The actin regulatory protein MENA, particularly its invasive isoform, MENA^{INV}, are established drivers of metastasis. MENA^{INV} expression is significantly correlated with metastasis and poor outcome in human breast cancer patients. We investigated whether MENA isoforms might play a role in driving resistance to chemotherapeutics. We find that both MENA and MENA^{INV} confer resistance to the taxane paclitaxel, but not to the widely used DNA damaging agents doxorubicin or cisplatin. Furthermore, paclitaxel treatment does not attenuate growth of MENA^{INV}-driven metastatic lesions. Mechanistically, MENA isoform expression alters the ratio of dynamic and stable microtubule populations in paclitaxel-treated cells. MENA expression also increases MAPK signaling in response to paclitaxel treatment. Decreasing ERK phosphorylation by co-treatment with MEK inhibitor restored paclitaxel sensitivity by driving microtubule stabilization in MENA isoform-expressing cells. Our results reveal a novel mechanism of taxane resistance in highly metastatic breast cancer cells and identify a combination therapy to overcome such resistance.

*Corresponding author: Frank B. Gertler, Koch Institute for Integrative Cancer Research, MIT 76-361a, 77 Massachusetts Ave, Cambridge, MA 02139, 617-253-5511, fgertler@mit.edu.

Disclosure of Potential Conflicts of Interest

F.B. Gertler has ownership interest (including patents) in MetaStat and is a consultant/advisory board member for the same. No potential conflicts of interest were disclosed by the other authors.

Introduction

While the number of targeted agents in clinical trials for metastatic breast cancer continues to increase, chemotherapy remains the standard of care for this disease, particularly for triple-negative breast cancer (TNBC), one of the most aggressive breast cancer subtypes (1). TNBC, defined by a lack of expression of both estrogen and progesterone receptor as well as low levels of HER2, accounts for 15% of breast tumors. TNBC is associated with a poorer prognosis along with a greater risk of recurrence and metastasis (2,3). Platinum agents, taxanes and anthracyclines are used in mono- or poly-chemotherapy as front line treatment, especially in the context of metastatic disease (4). Anti-mitotic chemotherapy agents generally target proliferating cancer cells, with platinum agents such as Cisplatin and anthracyclines including Doxorubicin primarily functioning through direct interaction with DNA and subsequent interference with its replication. In contrast, taxanes such as paclitaxel lead to mitotic catastrophe by stabilizing microtubules (MTs) and inhibiting their disassembly during metaphase, thus leading to mitotic arrest and cell death (5)(6). The benefits of cytotoxic chemotherapy for TNBC are clear; nevertheless, response rates are low, and over 50% of TNBC patients become resistant to chemotherapy typically by 6–10 months (7).

A number of cellular processes are known to drive chemo-resistance, which can arise from both cell intrinsic mechanisms as well as tumor microenvironment-driven external survival signals (8). First, changes in expression of the adenosine triphosphate-binding cassette (ABC) superfamily of transporters, in particular P-gp/MDR1, have been shown to be involved in paclitaxel resistance (9). While *in vitro* and pre-clinical studies showed increased cell death with dual chemotherapy and MDR1 inhibitor, the first and second generation of inhibitors both failed in clinical trials due to safety and efficacy issues (9). Second, mutations in a drug's cellular targets, β-tubulin in the case of taxanes, can drive cell intrinsic resistance by impairing paclitaxel binding, increasing MT dynamics, and blocking taxane-induced G2/M arrest (10). Third, changes in expression or function of proteins of the apoptosis pathways, such as caspase-3 or Bcl-2, have also been implicated in taxane resistance (11,12). Chemotherapy-induced pro-apoptotic signals can be counteracted by constitutive activation of the pro-survival PI3K/Akt/mTOR or RAF/RAS/MEK MAPK signaling pathways (13). Paclitaxel treatment can induce MAPK activation to attenuate MT stabilization (10), and multiple studies have demonstrated that co-treatment with paclitaxel and a MEK inhibitor can increase cancer cell death (14). Much of our understanding of these and other mechanisms of taxane resistance is derived from studies focused on cell survival and proliferation. The question of how such mechanisms of resistance are associated with cell invasion and metastatic disease itself remains understudied.

One key driver of breast cancer metastasis is MENA (also known as ENAH or hMena), a member of the Ena/VASP family of actin elongation factors that is upregulated in various cancer types, including breast cancer (15). MENA deficiency in the PyMT mouse model of breast cancer slows tumor progression and decreases metastasis (16), and stable depletion of MENA in the human breast adenocarcinoma MDA-MB-231 cells significantly decreases metastatic burden from orthotopic xenograft tumors (17). In addition to a broadly expressed 80kDa MENA isoform, multiple other MENA protein isoforms can arise in some cell types

from changes in the inclusion of 5 alternatively-spliced exons in the *MENA* mRNA (18–20). In human breast cancer patients and in mouse breast cancer models, changes in expression of two functionally distinct isoforms, MENA11a and MENA^{INV}, are linked to metastatic tumor cell phenotypes and to patient outcomes. MENA11a expression is high in normal epithelial tissues and in epithelial-like cells in breast cancer cells *in vitro* and *in vivo* (19,21), but is low in invasive tumor cell subpopulations (22). Mena11a suppresses tumor cell migration and invasion and promotes cohesive tumor morphology (19,21,23). While expression levels of either MENA or MENA11a alone do not correlate breast cancer patient outcome (17,24), patients with high Mena^{calc}, a measure of the total Mena levels minus MENA11a levels, have poor disease-specific survival (24,25).

In contrast to MENA11a, MENA^{INV} expression is significantly higher in metastatic compared to non-metastatic human breast tumors, and high levels of MENA^{INV}, but not MENA, are associated with increased metastasis and poor outcome in multiple human breast cancer cohorts (17). MENA^{INV} is highly upregulated in invasive tumor cell subpopulations *in vivo*, but found only at trace levels in even highly aggressive breast cancer cell lines in culture (22,26). Expression of MENA^{INV} in breast tumor cells renders them more sensitive to multiple pro-invasive growth factors (27,28) and increases their ability migrate towards higher concentration of fibronectin, which is especially abundant near blood vessels (17). As a consequence, cells expressing MENA^{INV} are more invasive and are highly metastatic. MENA^{INV} has been shown to drive resistance to targeted tyrosine kinase inhibitors in growth-factor elicited motility responses (28), however its role in regulating responses to chemotherapeutic drugs has never been studied. Chemotherapy regimens containing taxanes are the standard of care for patients with metastatic breast cancer(29). Given the fact that both MENA^{INV} and MENA are expressed in metastatic breast tumors and drive pro-metastatic phenotypes, we wondered whether expression of MENA and MENA^{INV} affected tumor cell responses to chemotherapy, and how, in turn, standard of care cytotoxic therapy might influence MENA/MENA^{INV}-driven metastasis. We show, using *in vitro* and *in vivo* models, that highly metastatic cells expressing MENA or MENA^{INV} confer paclitaxel resistance, by preventing the MT stabilization via activation of the MAPK signaling cascade. Our findings reveal a novel mechanism by which highly metastatic breast cancer cells can become resistant to taxanes.

Materials and methods

Antibodies and drugs

Antibodies—The anti-MENA and anti-MENA^{INV} antibodies were generated in the laboratory and previously described (30,26), anti-tubulin (Sigma, DM1A), anti-tubulin detyrosinated or Glu-Tubulin (Millipore, AB3201), anti-tubulin tyrosinated (Millipore, ABT171), anti-pERK Y204 (Santa Cruz, sc7383), anti-GAPDH (Sigma, G9545), anti-Ki67 (BD Biosciences), cleaved Caspase-3 (BD Biosciences), anti-pAkt473 (CST).

Drugs—Doxorubicin, Cisplatin and paclitaxel (Sigma), Docetaxel. For *in vitro* experiment, drugs were diluted in cell culture media with 1% of DMSO. Vehicle control correspond to

cells treated with culture media with 1% of DMSO (no drug), PD0325901 MEK inhibitor (LC Labs), MDR1 inhibitor HM30181 (100nM) gift from the Weissleder Lab (MGH)(31).

Cell Culture

MDA-MB-231 cells were purchased directly from the ATCC in June 2012, where cell lines are authenticated by short tandem repeat profiling. These cells were not reauthenticated by our lab and were cultured in DMEM with 10% FBS (Hyclone). Cell line generation and FACS were performed as previously described (32). Cell lines show a 8- to 10-fold overexpression relative to endogenous MENA, and are labeled 231-Control, 231-MENA and 231-MENA^{INV} (17). SUM159 cells were obtained from Joan Brugge's lab at Harvard Medical School (January 2011) and were not reauthenticated in our lab. SUM159 cells were cultured according to the ATCC protocols. T47D cells were purchased at ATCC, where cell lines are authenticated by short tandem repeat profiling. They were cultured according to the manufacturer's protocol, and not reauthenticated in our lab. Stable Knockdown cell lines (T47D) were generated using using a retroviral vector to express a mir30-based shRNA sequence 'CAGAAGACAATCGCCCTTTAA' targeting a sequence shared amongst all known Mena mRNA isoforms. By western blot analysis detected using an anti-Mena monoclonal that recognizes an epitope shared in all known Mena protein isoforms (33) indicated that expression of all molecular species detected were significantly reduced in the T47D-ShMena cell line; expression analysis of specific MENA isoforms was not performed. MDA-MB 175IIV, MDA-MB 453, MDA-MB 436, BT-549, LM2 and BT-20 were gifted by Dr Michael Yaffe's lab (Koch Institute, MIT) in April 2015, and cultured according manufacturer's protocol, and not reauthenticated by our lab.

Cell viability assay

Cell viability assays were performed in a 96-well plate. 5,000 cells were plated per well and treated with drug 24h later. Cell viability was assayed 72 hours later using the PrestoBlue Cell Viability Reagent (Life Technologies), according to manufacturer's protocol. Fluorescence was measured and normalized to cells exposed to vehicle. The activity area was calculated from dose–response plots using Matlab. All measurements were repeated in triplicate.

Xenograft tumor generation and *in vivo* chemotherapy treatment

All animal experiments were approved by the MIT Division of Comparative Medicine. 2 million MDA-MB-231 cells expressing different MENA isoforms (in PBS and 20% collagen I) were injected into the 4th right mammary fat pad of six week-old female NOD-SCID mice (Taconic). When the tumors reached 1 cm in diameter, mice were treated every five days with either three doses of paclitaxel at 10mg/kg in 1% DMSO, 3% PEG (MW 400), 1% Tween 80 in PBS by intra-peritoneal injection. In parallel, mice were treated with only in 1% DMSO, 3% PEG (MW 400), 1% Tween 80 in PBS as a vehicle control. One day after the last injection, tumors were measured and mice were use for intravital imaging and then sacrificed. Their tumors and lungs were fixed in 10% formalin overnight, their bone marrow were collected using PBS and cultured in DMEM with 10% fetal bovine serum. The number of tumor cell colonies in cultured bone morrow was counted 1 month after collection. The number of metastasis in each lobe of the lung were counted from lung H&E stained sections

visualized by light microscopy and counted by two blinded individuals. Each tumor group contained 3–5 mice.

Intravital imaging

Intravital multiphoton imaging was performed as described previously (17) using a 25x 1.05 NA water immersion objective with correction lens. After exposing the tumor with a skin flap surgery, 30 min movies were captured. The number of motile cells in each field of view were count in ten 30 min time-lapse movies using ImageJ. Motile cells were cells who show any displacement of the nucleus and cell protrusion activity. Data were pooled from 2–4 mice per tumor group, with 4–10 fields imaged per mouse.

Western blot

Cells were lysed in 25mM Tris, 150mM NaCl, 10% glycerol, 1% NP 40 and 0.5M EDTA with a protease Mini-complete protease inhibitors (Roche) and a phosphatase inhibitor cocktail (PhosSTOP, Roche) at 4°C for 20 min. Protein lysates were separated by SDS-PAGE, transferred to a nitrocellulose membrane and blocked with Odyssey Blocking Buffer (LiCor). Membranes were incubated with primary antibody overnight at 4°C and Licor secondary antibodies at room temperature for 1 hour. Protein level intensity was measured with Image J.

Immunohistochemistry

Tumors dissected from NOD/SCID mice were fixed in 10% buffered formalin and embedded in paraffin. Tissue sections (5μm thick) were deparaffinized followed by antigen retrieval using Citra Plus solution (Biogenex). After treatment with 3% H_2O_2, sections were blocked with serum, incubated with primary antibodies overnight at 4°C and fluorescently labeled secondary antibodies at room temperature for 2 hrs. Sections were stained using anti-MENA (1:500), biotinylated anti-MENA^{INV} (1:500), anti-CC3 (1:200), anti-Ki67 (1:200) and DAPI. Fluorochromes on secondary antibodies included AlexaFluor 488, 594 or 647 (Jackson Immunoresearch). Sections were mounted in Fluoromount mounting media and imaged at room temperature. Z series of images were taken on a DeltaVision microscope using Softworx acquisition, an Olympus 40x 1.3 NA plan apo objective and a Photometrics CoolSNAP HQ camera. At least 10 fields were captured for each tumor, with at least 3 tumors per tumor group.

Human breast cancer expression analysis

Data retrieval from TCGA(34) (Fig S1A,B) was explained in (17). The data for MENA^{INV} protein levels as measure by immunohistochemistry are also in (17), from patient samples obtained from (35).

In vitro imaging

Glass bottom dishes were coated with Collagen at 0.1 mg/ml diluted in PBS for 1 hour at 37°C. Cells expressing different MENA isoform were treated with paclitaxel at 1, 10 or 100 nM or vehicle and immediately plated on the glass bottom dishes. 30 min later, cells were imaged overnight, with one image acquired every 10 min for 16 hours on a Nikon spinning

disk with a 20X objective and an Andor/NeoZyla camera. Individual cells were manually tracked using ImageJ and Manual Tracking plug-in. Data were analyzed using the chemotaxis tool developed by IBIDI. For analysis of time spent in cell division, we measured the time between when the mother cell first rounds up, to when both daughter cells have spread out on substrate. The percentage of successful cell divisions was quantified by counting the number of cell divisions that lead to two surviving daughter cells. Data are pooled from at least 50 cells tracked in three independent experiments.

Cell cycle analysis

231-Control, 231-MENA and 231-MENA^{INV} cells were treated with paclitaxel at 10nM or 100nM or vehicle. After 16h of treatment, cells were trypsinized, wash in cold PBS, centrifuged at 1000 rpm for 3 min, resuspended in 1ml of ice cold PBS, fixed by adding 4 ml of ethanol at −20°C, and incubated at 4°C for 1 hour. After fixation, cells were washed with ice-cold PBS and centrifuged at 22,000 rpm for 20 min. DNA was stained using Propidium iodine at 50μg/ml and RNase A at 1mg/ml for 30 min at 37°C. DNA content was measured on a FACSCalibur cytometer (Becton-Dickinson California). Data were analyzed using Modfit software (Verity Software House), with appropriate gating on the FL2-A and FL2-W channels to exclude cell aggregates. 25,000 events were analyzed per sample.

Immunofluorescence

Glass bottom dishes (Mattek) were coated with Collagen at 0.1 mg/ml diluted in PBS and 50 μg/ml FN for 1 hour at 37°C. Cells were plated for 1hr, and then treated with paclitaxel alone or in combination with MEKi for 24h. Cells were fixed for 20 min in 4% paraformaldehyde in PHEM buffer with 0.1% Gluteraldehyde, and then quenched with sodium borohydrate for 5mins. Cells were blocked with 2% BSA in TBS-0.1%TritonX-100 for 30 mins, and incubated with primary antibodies and then secondary antibodies for 1hr each, at room temperature. Z series of images were taken on an Applied Precision DeltaVision microscope using Softworx acquisition, an Olympus 60x 1.4 NA plan apo objective and a Photometrics CoolSNAP HQ camera. Images were deconvolved using Deltavision Softworx software and objective specific point spread function. Images were analyzed with ImageJ, where the whole cell intensity levels of Tyr- or Glu-MT was measured. Images are pooled from at least 3 independent experiments.

MT length image analysis

MT images were processed with 1) a filament reconstruction algorithm that selects bona fide filaments and 2) a post-analysis that quantifies the properties of the MT network organization. For the filament reconstruction, briefly, the MT images were first filtered by multiple-scale steerable filter to enhance the curvilinear features. From the filtered images, the centerlines of possible filament fragments were detected and separated into high and low confidence sets. Some of low confidence filament fragments were linked to high confident fragments using iterative graph matching. The output of the reconstruction is a network of filaments each presented by an ordered chain of pixels and the local filament orientation. The MT length was calculated as the number of pixels converted to microns, per each identified filament. Overall, at least 2000 MTs were analyzed per condition, from at least two experiments.

Results

MENA and MENA^{INV} are associated with increased survival during paclitaxel treatment *in vitro*

To investigate a potential role for MENA in resistance to chemotherapy in breast cancer, we first asked whether endogenous MENA and MENA^{INV} expression levels were associated with paclitaxel resistance. MENA and MENA^{INV} are widely expressed in all main breast cancer subtypes, as measured by mRNA from TCGA samples, as well as at the protein level by immunohistochemistry(17) (FigS1A–C), with slightly higher expression in patients with Her2+ breast cancer. We then measured paclitaxel efficacy and quantified levels of endogenous MENA protein expression across cell lines from several human breast cancer types, including: Luminal A (MDA-MB 175IIV and T47D), HER2 positive (MDA-MD 453) and TNBC (SUM 159, BT-20, MDA-MB 436, LM2, BT-549, MDA-MB 231) (Fig 1A,B, Fig S1D). In addition to the canonical 80kDa MENA isoform, some the cell lines used express other MENA isoforms endogenously, such as MENA11a, which is known to be expressed in epithelial-like cell lines including T47D cells and absent from mesenchymal-like cell lines including BT-549 and MDA-MB-231 cells. Under the conditions we used, MENA11a co-migrates with the 80kDa MENA, thus the intensity of the measured the 80kDa MENA, detected with an antibody known to recognize all MENA isoforms, represents the total amount of 80kDa MENA plus MENA11a in the cell lines that express both isoforms. There was a significant inverse correlation between paclitaxel efficacy, as measured by cell survival, and levels of endogenous MENA expression (Fig 1C). To confirm that endogenously-expressed MENA promotes Paclitaxel resistance, we knocked down MENA in T47D cells, which normally express MENA and MENA11a (Fig S1E)(19,21). It is important to note that the shRNA used for these experiments targets a sequence common to all known MENA isoforms, thereby depleting MENA11a as well as MENA. Reducing all MENA isoform levels (> 75%) in T47D cells renders them more sensitive to Paclitaxel (Fig 1D).

To study the role of MENA and MENA^{INV} independently, we used a triple-negative breast adenocarcinoma cell line (MDA-MB-231), which endogenously expresses low levels of MENA and, like other cultured breast cancer cell lines only trace levels of MENA^{INV} *in vitro*. As endogenous Mena^{INV} expression is highly upregulated by aggressive tumor cells within the *in vivo* tumor microenvironment (17,22,26), we stably over-expressed GFP (231-Control), GFP-tagged MENA (231-MENA) or MENA^{INV} (231-MENA^{INV}) at equivalent levels in this cell line to match the robust expression observed *in vivo*. We observed that the fraction of viable 231-MENA or 231-MENA^{INV} cells was at least 65% higher than the fraction of viable 231-Control cells, after 72h of treatment with varying doses paclitaxel (Fig1E). To investigate the specificity of the response, we also tested two other commonly used chemotherapeutics, doxorubicin and cisplatin, and found that neither MENA nor MENA^{INV} expression affected the response to the different concentrations of either drug (Fig S1F,G). These experiments revealed that cell viability in the presence of high paclitaxel concentrations is decreased with low MENA expression and increased by ectopic expression of MENA or MENA^{INV}. These data suggest that the increased levels of MENA isoforms

observed in tumor cells during metastatic progression may contribute to paclitaxel resistance.

MENA isoform expression is associated with increased tumor growth *in vivo* during paclitaxel treatment

We then investigated whether MENA-associated paclitaxel resistance could also be observed *in vivo*. Xenograft tumors were generated by injecting MDA-MB-231 cells expressing MENA isoforms into the mammary fat pads of NOD-SCID mice. Mice were treated with paclitaxel once tumors reached 1cm in diameter (Fig 2A). Treatment with paclitaxel significantly decreased the growth of 231-Control tumors compared to mice treated with vehicle (Fig 2B). However, the growth of 231-MENA or 231-MENA^{INV} tumors was unaffected by paclitaxel treatment (Fig 2B), thereby suggesting MENA and MENA^{INV} promote drug resistance *in vivo*.

The increased size of paclitaxel-treated 231-MENA and 231-MENA^{INV} tumors could arise from elevated levels of proliferation, decreased levels of cell death, or both. We evaluated proliferation and apoptosis by quantifying the intensity of cells positive for Ki67 and CC3, respectively by immunostaining. Although paclitaxel treatment decreased the amount of Ki67 staining in 231-Control tumors, it failed to decrease the numbers of Ki67-positive cells in 231-MENA and 231-MENA^{INV} tumors (Fig 2C,D). In contrast, treatment did lead to an increase in cell death as marked by CC3 positive cells in all tumors (Fig 2E,F). These data indicate that during paclitaxel treatment of tumor bearing animals, MENA or MENA^{INV} expressing tumor cells continue to proliferate, but exhibit similar rates of apoptosis to control tumors.

Paclitaxel treatment decreases cell velocity *in vitro,* but does not affect MENA^{INV}-driven tumor cell motility and dissemination in mice

MENA and MENA^{INV} drive increased cell motility and metastasis during tumor progression (17,27). Therefore, we examined whether MENA isoform expression impacts cell migration and dissemination after paclitaxel treatment. *In vitro*, paclitaxel treatment decreased velocity of the three MENA isoform expressing cell lines (Fig S2). However, at every concentration of the drug used, 231-MENA^{INV} maintained higher velocity than cells expressing MENA or control cells. Using multiphoton intravital imaging we found that, *in vivo*, paclitaxel treatment significantly reduced the number of cells moving within 231-Control tumors. On the contrary, motility of 231-MENA and of 231-MENA^{INV} tumor cells was not affected by the treatment (Fig 3A). To investigate the effect of paclitaxel treatment on metastatic burden, we counted the number of colonies in cultured bone morrow and the number of metastases in the lung from mice bearing 231-Control, 231-MENA or 231-MENA^{INV} tumors for 12 weeks. Neither the number of bone marrow colonies (Fig 3B), nor the number of lung metastases (Fig 3C,D) from 231-MENA or 231-MENA^{INV} tumors were affected by treatment with paclitaxel. These data suggest that highly metastatic cells, such as those expressing MENA isoforms, are not affected by paclitaxel treatment in the context of metastatic disease.

Paclitaxel treatment selects for high MENA expression *in vitro* and *in vivo*

Our results so far indicated that increased MENA or MENA^{INV} expression levels are associated with reduced responses to paclitaxel. We next investigated the effect of paclitaxel treatment on levels of MENA expression in cell populations *in vitro* and *in vivo*. First, we analyzed endogenous MENA expression by Western Blot in 5 breast cancer cell lines that were exposed to 100nM of paclitaxel or a vehicle control (Fig 4A). We found that 72h after paclitaxel treatment, some cell lines (MDA-MB-231 and MDA-MB-175VII) showed increased MENA expression (Fig 4B). We performed a similar analysis using MDA-MB-231 cell populations expressing heterogenous levels of either GFP, GFP-MENA or GFP-MENA^{INV}. FACS analysis revealed that treatment with Docetaxel (a taxane closely related to paclitaxel) selected for cells expressing higher levels of GFP-MENA or GFP-MENA^{INV}, but not of GFP (Fig 4C). Finally, quantitative immunofluorescence analysis of tissue sections from 231-Control tumors taken from animals that were treated with either paclitaxel or a vehicle control revealed significant increases in total MENA levels, detected by a pan-MENA antibody, and in MENA^{INV} levels, detected by an anti-MENA^{INV} isoform specific antibody, in tumors from the paclitaxel-treated mice compared to vehicle (Fig 4D–F). Together, these data indicate that, both *in vitro* and *in vivo*, paclitaxel treatment selects for tumor cells cells expressing a higher level of MENA and MENA^{INV}.

MENA isoform-driven resistance does not involve drug efflux or focal adhesion signaling, but does affect cell division

We next investigated the mechanism by which MENA and MENA^{INV} increase resistance to paclitaxel. Paclitaxel efflux through the MDR1 pump is one of the most frequent and best described mechanisms of paclitaxel resistance (9). Co-treatment with HM30181, a 3rd generation MDR1 inhibitor (31), and 100nM of paclitaxel negligibly affected the fraction of viable 231-Control cells and did not increase paclitaxel efficacy in 231-MENA^{INV} cells (Fig S3A). Focal adhesion signaling has been reported to promote resistance to paclitaxel (36), and we previously reported that MENA regulates focal adhesion signaling via a direct between an LERER-repeat domain in MENA and the cytoplasmic tail of α5 integrin (32). To determine whether the interaction between MENA and α5 is required for increased resistance to paclitaxel, we assayed cells expressing α5-binding deficient versions of MENA or MENA^{INV} (lacking the LERER-repeat domain) and found that these mutants versions were equally effective to the wild type versions in increasing resistance to paclitaxel (Fig S3B). These data indicate that neither drug efflux, nor the MENA-α5 interaction mediate MENA isoform-driven resistance to paclitaxel.

One of the key steps in paclitaxel-induced cell death is cell arrest in the G2/M phases of the cell cycle. We performed cell cycle analysis on 231-Control, 231-MENA and 231-MENA^{INV} cells treated with 10nM or 100nM of paclitaxel for 16h (Fig S4A–C), and found a similar dose-dependent increase of cells in the G2/M phase across all three cell lines. Therefore, MENA or MENA^{INV} expression does not impair paclitaxel-induced arrest in G2/M, as measured in cells in suspension by flow cytometry. We next performed time-lapse microscopy to study the cell division phenotypes in more detail, and imaged cells expressing MENA isoforms while adherent on collagen (Fig S4D–F). Treatment with paclitaxel increased the time 231-Control cells spent rounded in cell division by four-fold, however,

231-MENA and 231-MENA^{INV} showed only a two-fold increase in the time spent in cell division (Fig S4G). Furthermore, paclitaxel treatment led to a 40% decrease in the number of successful divisions in 231-Control cells, in which one cell divides into two surviving daughter cells (Fig S4H). In contrast, over 90% of cells divisions in paclitaxel treated 231-MENA and 231-MENA^{INV} cells were successful (Fig S4H). Together, these data suggest that MENA isoform expression confers the ability to progress through cell division more effectively and successfully during treatment with paclitaxel.

Expression of MENA is associated with increased ratio of dynamic to stable MTs during paclitaxel treatment

Paclitaxel promotes cell death by increasing the stability of MTs, and pathways driving increased MT dynamics are known to promote resistance to taxanes (10). Therefore, we examined MT structure and dynamics in MENA isoform expressing cells during paclitaxel treatment. We found that at baseline, 231-MENA and 231-MENA^{INV} cells contained longer MTs (Fig S5A–C). Paclitaxel treatment had no effect on MT length in either 231-Control or 231-MENA cells, but did elicit a small but significant increase in 231-MENA^{INV} cells (Fig S5C). Post-translational modification of MTs can regulate their dynamics, and antibodies that detect such modifications can be used to infer the relative dynamics of MT populations; in particular, MT tyrosination indicates a dynamic MT state, while de-tyrosination of MTs is associated with increased stability (37). We measured the relative abundance of stable (Glu-MT) vs. dynamic (Tyr-MT) MTs in individual cells by immunofluorescence with anti-Glu-MT and anti-Tyr-MT antibodies (Fig 5A,B). In 231-Control cells, treatment with paclitaxel led to a significant increase in the relative ratio of stable to dynamic MTs. However, in both 231-MENA and 231-MENA^{INV} cells, there was no change in the relative levels of stable to dynamic MTs (Fig 5C). Together, these data demonstrate that MENA isoforms can affect MT length, and that MENA isoform expression maintains dynamic MTs during paclitaxel treatment.

MENA drives resistance to paclitaxel by increasing MAPK signaling

The MAPK signaling cascade is among the key pathways known to interact with MTs. Both ERK1/2 interact with MTs; MT stabilization by paclitaxel increases ERK phosphorylation and, in turn, ERK pathway activation increases MT dynamics (10). We measured levels of ERK phosphorylation in 231-Control, 231-MENA and 231-MENA^{INV} cell lines after 72h of paclitaxel treatment. We found that 231-MENA and 231-MENA^{INV} cells had higher levels of pERK Y204 relative to 231-Control cells, after paclitaxel treatment, while total ERK levels were unchanged in the same conditions (Fig 6A,B, Fig S6A,B). In contrast, treatment with paclitaxel decreased pAkt473 levels equally in all three cell lines, without significantly changing total Akt levels (Fig S6 C–F). We therefore asked whether MEK inhibition (MEKi) could make MENA isoform expressing cells more sensitive to paclitaxel. In all cell lines, we found significant additive effects between paclitaxel and MEKi PD0325901 in a proliferation assay (Fig 6C–E), where treatment with both drugs simultaneously led to a greater increase in cell death than with each drug alone. However, higher concentrations of each drug were needed in 231-MENA and 231-MENA^{INV} cells to obtain high levels of cell death, relative to 231-Control cells. MEKi treatment blocked paclitaxel-induced ERK phosphorylation in 231-MENA^{INV} cells (Fig 6F). Finally, we investigated the effect of

paclitaxel and MEKi treatment on MT dynamics in 231-MENA^{INV} cells and found that treatment with both drugs simultaneously induced increases in stable MTs relative to dynamic MTs, while treatment with either drug alone had no effect (Fig 6G,H). Together, these data suggest that MENA isoforms drive resistance to paclitaxel via sustained MT dynamics and increased ERK signaling.

Discussion

Previous work has identified several MENA isoforms, in particular MENA^{INV}, as key drivers of metastatic breast cancer, with high MENA^{INV} levels being associated with increased recurrence and poor outcome in breast cancer patients (17). Our data highlight an additional, unexpected role for MENA and MENA^{INV} in driving resistance to paclitaxel by maintaining dynamic MTs during paclitaxel treatment. We found that MENA and MENA^{INV} expression maintains MT dynamics during paclitaxel treatment, leading to increased MAPK signaling. While taxanes remain the standard of care for metastatic breast cancer, our data suggest this class of drugs may not be as effective in targeting certain highly invasive, metastatic cells.

We observed an inverse correlation between the levels of endogenous MENA expression in cultured breast cancer cell lines and sensitivity to paclitaxel. Ectopic expression of MENA or MENA^{INV} in cultured MDA-MB-231 cells, which have low levels of endogenous MENA, decreased sensitivity to paclitaxel. Conversely, in T47D cells, which endogenously express high levels of MENA and MENA11a, depletion of all MENA isoforms increased sensitivity to paclitaxel. Together these data indicate that MENA expression promotes resistance to paclitaxel. Since MENA11a as well as MENA is expressed T47D and some of the other cell lines in our analysis, it is possible that MENA11a can contribute to paclitaxel resistance, though we did not perform any experiments to address whether or not MENA11a plays a functional role in resistance to paclitaxel. In this context, however, it is of interest to note that, while a role for MENA11a in resistance to chemotherapy remains unknown, MENA11a expression contributes to resistance to PI3K inhibitors in HER-2 overexpressing breast cancer cells (38). While beyond the scope of this study, it will be interesting to determine the extent to which other MENA11a and other MENA isoforms may contribute to paclitaxel resistance, and how taxane therapy may affect expression of all MENA isoforms in patients.

Superficially, it may seem paradoxical that aggressive breast cancer cell lines such as MDA-MB-231 and BT549, which express low levels of endogenous MENA and only trace levels of MENA^{INV} when cultured *in vitro*. Our previous results indicate that MENA and MENA^{INV} expression is upregulated significantly in aggressive tumor cell subpopulations when cultured breast cancer cells are implanted to make orthotopic tumors in immunocomprised mice (22). Therefore, it is likely that growth in the tumor microenvironment triggers changes in gene expression and alternative splicing in xenografted cells that increase the abundance of MENA and MENA^{INV} during tumor progression, similar to the what is observed in autochtonous mouse mammary carcinomas and human breast tumors(26). As our goal in this study was to determine investigate how MENA isoform expression might affect breast cancer patients with aggressive, potentially metastatic disease, we designed our experiments based on knowledge derived from studies

of MENA isoform expression in tumor cells *in vivo*. To mimic the effect of the tumor microenvironment on MENA isoform expression for analyses *in vitro*, we engineered MDA-MB-231 cells to express MENA or MENA^{INV}, the two isoforms expressed in patients with aggressive, metastatic breast cancer. Our experiments demonstrated that MENA isoforms expressed in metastastic tumors confer resistance to paclitaxel, and, conversely, that paclitaxel treatment results in increased expression of MENA and MENA^{INV} in tumors. Since we found that paclitaxel treatment was less effective in reducing metastatic burden in tumors with elevated MENA^{INV}, it is possible that taxane-based therapy may, in some cases, trigger elevated expression MENA^{INV} expression that, in turn, both promotes metastasis and decreases the efficacy of the treatment. Studies to invesitigate this possibility are underway.

How might MENA/MENA^{INV} promote resistance to taxanes? We initially hypothesized that MENA's role in regulating focal adhesion (FA) signaling may be important in this context, given the established links between FAs and MTs (39), as well as the known abundance of MENA at FA sites and its direct interaction with the α5 integrin subunit (17,32). We found, however, that interaction with α5 was not required MENA-dependent increases in taxane resistance (Fig S2). After paclitaxel treatment, MENA-expressing cells showed an increase in the abundance of dynamic MT populations, in paclitaxel-treated cells (Fig 5). Therefore, it will be interesting to understand whether MENA influences MTs via association with MT-binding proteins, through an effect on signaling pathways that regulate MT dynamics, or both.

Interestingly, under control conditions, our data show that MENA or MENA^{INV} expression increased MT length, support a role for MENA in regulation of MT behavior (Fig S4). Consistent with these findings, siRNA depletion of *Enabled* (*Ena*), the sole *Drosophila* MENA ortholog (18) in *Drosophila* S2 cells induced significant changes in MT dynamics, suggesting a potentially evolutionarily conserved role for MENA in regulating MT dynamics. However, under control conditions, we did not detect any changes in tyrosination at the whole cell level, which may be due to the fact that whole cell immunofluorescence is not sensitive enough to detect subtle differences (Fig 5). It is clear, however, that some actin regulatory proteins can regulate MT dynamics. For example, formins, actin nucleating and elongation factors, can also act as positive regulators of MT organization and stability (40). For example, complexes containing the activated forms of the formins mDia1 and INF2 along with the scaffolding, and MT-binding protein IQGAP1 can increase MT stabilization via direct interaction with MTs (41), and MT regulators can also influence formin-dependent actin dynamics (42). Interestingly, a genetic screen in Drosophila identified *Ena* as a dosage-sensitive modifier of phenotypes associated with ectopic expression of the MT +TIP tracking protein CLASP (43). Therefore, future work focused on the interplay between the actin-based cell motility machinery and MT regulation using fluorescent reporters for MT tip proteins coupled to live imaging may yield additional insight into the acquisition of taxane resistance by metastatic cancer cells.

Paclitaxel resistance driven by MENA isoforms leads to sustained MT dynamics that, in turn, lead to increased ERK signaling, at least *in vitro* (Fig 6). Disruption of MT dynamics can lead to ERK phosphorylation, and MAPK activation can inhibit MT stabilization (14,44,45). Therefore, a feedback mechanism may act to balance MAPK pathway activity

with MT dyanmics. Our data indicating that combined treatment with paclitaxel and MEKi, but not with either drug individually, leads to increased MT stability in MENA^{INV} cells, raises the possibility that MENA^{INV} alters the balance between MAPK singaling and MT dynamics (Fig 6). In a breast cancer cohort, MENA expression, as assessed by IHC, correlated with pERK and pAkt staining, with a higher number of pERK and pAkt positivity in MENA-positive tumors, irrespective of Her-2 status (46). Depletion of all MENA isoforms in the MCF7 Her2-overpressing line decreased ERK signaling, and inhibited EGF/NRG1 mediated effects on cell proliferation (46). These data are consistent with a potential role for MENA in regulating ERK signaling. Alternatively, activation of bypass signaling pathways such as the Akt pathway, occurs downstream of integrins in response to paclitaxel treatment, even in the absence of differences in G2/M arrest (47). Interestingly, there were no MENA-isoform induced differences in the levels of Akt phosphorylation (Fig S6), which were significantly decreased in all three cell lines, during paclitaxel treatment. This finding is also consistent with our *in vivo* data showing that during paclitaxel treatment, MENA isoform expression selectively increases proliferation, which is relatively more senstive to MAPK signaling, but not apoptosis, which is relatively more sensitive to Akt signaling. Finally, our data suggest that combined treatment with a taxane with a MEKi could bypass MENA-isoform driven resistance (Fig 6). Several groups have previously shown that treatment with a MEKi can enhance paclitaxel-driven cell death *in vitro* and *in vivo* (48–50). Multiple clinical trials are currently underway in advanced solid tumors, such as melanoma and non-small cell lung cancer, testing combinations of taxanes and the MEK inhibitor Trametinib (51).

Our data reveal an interesting relationship between the response of highly metastatic cells to taxanes, as well as the effect of taxanes on highly metastatic cell populations in tumors, that could have important clinical implications. First, following paclitaxel treatment, MENA and MENA^{INV} protein expression was higher in both *in vitro* and in xenograft tumors, suggesting that residual surviving cells have undergone a selection for increased MENA and MENA^{INV} levels (Fig 4). Second, we found that MENA^{INV}-driven tumor cell motility and metastasis is not affected by paclitaxel treatment (Fig 3). Paclitaxel is widely used as adjuvant therapy to prevent breast tumor relapse and metastasis (52). Our data suggest that paclitaxel may be less effective in treating patients that have primary tumors expressing high levels of MENA^{INV}. While here we focused on triple-negative breast cancer, reduction in MENA levels in ER+ breast cancer cells also altered sensitivity to Paclitaxel (Fig 1), raising the possibility that this mechanism may be important in other subtypes. Currently, there are no biomarkers that predict response to taxanes in patients (53). MENA isoforms are being developed as biomarkers in breast cancer to predict metastatic potential and to guide patient treatment (54). We also recently developed a MENA^{INV} isoform specific antibody and used it to demonstrate that metastatic tumors express higher MENA^{INV} than non-metatastic primary tumors, and that high MENA^{INV} protein levels were significantly associated with poor outcome and recurrence in a breast cancer patient cohort (17,26). While further work is needed to establish a clear link between MENA^{INV} expression and resistance to paclitaxel in patients, it will be interesting to study how paclitaxel increases MENA^{INV} expression and whether this may contribute to a more aggressive phenotype in post-treatment residual tumor cell populations.

Supplementary Material

Refer to Web version on PubMed Central for supplementary material.

Acknowledgments

Financial support:

This work was supported by a DoD Breast Cancer Research Program post-doctoral fellowship (W81XWH-12-1-0031), a Ludwig post-doctoral fellowship and K99-CA207866-01 to M. J. Oudin, ENS-Cachan funds to L. Barbier, funds from the Ludwig Center at MIT to FBG, NIH grant U54-CA112967 to F.B. Gertler and D.A. Lauffenburger, the Koch Institute Frontier Award from the Kathy and Curt Marble Research Fund to F. B. Gertler and O. Jonas, the Koch Institute NCI core grant P30-CA14051 to all authors.

References

1. Zardavas D, Baselga J, Piccart M. Emerging targeted agents in metastatic breast cancer. Nat Rev Clin Oncol. 2013; 10:191–210. [PubMed: 23459626]
2. Perou CM, Sørlie T, Eisen MB, van de Rijn M, Jeffrey SS, Rees Ca, et al. Molecular portraits of human breast tumours. Nature. 2000; 406:747–52. [PubMed: 10963602]
3. Dent R, Hanna WM, Trudeau M, Rawlinson E, Sun P, Narod SA. Pattern of metastatic spread in triple-negative breast cancer. Breast Cancer Res Treat. 2009; 115:423–8. [PubMed: 18543098]
4. Isakoff SJ. Triple Negative Breast Cancer: Role of Specific Chemotherapy Agents. cancer J. 2010; 16:53–61. [PubMed: 20164691]
5. Jordan, Ma. Mechanism of action of antitumor drugs that interact with microtubules and tubulin. Curr Med Chem Anticancer Agents. 2002; 2:1–17. [PubMed: 12678749]
6. Kaufmann SH, Earnshaw WC. Induction of apoptosis by cancer chemotherapy. Exp Cell Res. 2000; 256:42–9. [PubMed: 10739650]
7. Gluz O, Liedtke C, Gottschalk N, Pusztai L, Nitz U, Harbeck N. Triple-negative breast cancer—current status and future directions. Ann Oncol. 2009; 20:1913–27. [PubMed: 19901010]
8. Longley DB, Johnston PG. Molecular mechanisms of drug resistance. J Pathol. 2005; 205:275–92. [PubMed: 15641020]
9. Szakács G, Paterson JK, Ludwig Ja, Booth-Genthe C, Gottesman MM. Targeting multidrug resistance in cancer. Nat Rev Drug Discov. 2006; 5:219–34. [PubMed: 16518375]
10. Orr GA, Verdier-Pinard P, McDaid H, Horwitz SB. Mechanisms of Taxol resistance related to microtubules. Oncogene. 2003; 22:7280–95. [PubMed: 14576838]
11. Wang S, Wang Z, Boise L, Dent P, Grant S. Loss of the bcl-2 phosphorylation loop domain increases resistance of human leukemia cells (U937) to paclitaxel-mediated mitochondrial dysfunction and apoptosis. Biochem Biophys Res Commun. 1999; 259:67–72. [PubMed: 10334917]
12. Siddik ZH. Cisplatin: mode of cytotoxic action and molecular basis of resistance. Oncogene. 2003; 22:7265–79. [PubMed: 14576837]
13. Miller TW, Rexer BN, Garrett JT, Arteaga CL. Mutations in the phosphatidylinositol 3-kinase pathway: role in tumor progression and therapeutic implications in breast cancer. Breast Cancer Res. 2011; 13:224. [PubMed: 22114931]
14. McDaid HM, Horwitz SB. Selective potentiation of paclitaxel (taxol)-induced cell death by mitogen-activated protein kinase kinase inhibition in human cancer cell lines. Mol Pharmacol. 2001; 60:290–301. [PubMed: 11455016]
15. Gertler F, Condeelis J. Metastasis: tumor cells becoming MENAcing. Trends Cell Biol. 2011; 21:81–90. [PubMed: 21071226]
16. Roussos ET, Wang Y, Wyckoff JB, Sellers RS, Wang W, Li J, et al. Mena deficiency delays tumor progression and decreases metastasis in polyoma middle-T transgenic mouse mammary tumors. Breast Cancer Res BioMed Central Ltd. 2010; 12:R101.

17. Oudin, MJ., Jonas, O., Kosciuk, T., Broye, LC., Guido, BC., Wyckoff, J., et al. Tumor cell-driven extracellular matrix remodeling enables haptotaxis during metastatic progression. Cancer Discov. 2016. Available from: http://www.ncbi.nlm.nih.gov/pubmed/26811325
18. Gertler FB, Niebuhr K, Reinhard M, Wehland J, Soriano P. Mena, a relative of VASP and Drosophila Enabled, is implicated in the control of microfilament dynamics. Cell. 1996; 87:227–39. [PubMed: 8861907]
19. Di Modugno F, Iapicca P, Boudreau A, Mottolese M, Terrenato I, Perracchio L, et al. Splicing program of human MENA produces a previously undescribed isoform associated with invasive, mesenchymal-like breast tumors. Proc Natl Acad Sci U S A. 2012; 109:19280–5. [PubMed: 23129656]
20. Di Modugno F, Demonte L, Balsamo M, Bronzi G, Nicotra MR, Alessio M, et al. Molecular Cloning of hMena (ENAH) and Its Splice Variant hMena+11a: Epidermal Growth Factor Increases Their Expression and Stimulates hMena+11a Phosphorylation in Breast Cancer Cell Lines. Cancer Res. 2007; 67:2657–65. [PubMed: 17363586]
21. Balsamo M, Mondal C, Carmona G, McClain LM, Riquelme DN, Tadros J, et al. The alternatively-included 11a sequence modifies the effects of Mena on actin cytoskeletal organization and cell behavior. Sci Rep. 2016; 6:35298. [PubMed: 27748415]
22. Goswami S, Philippar U, Sun D, Patsialou A, Avraham J, Wang W, et al. Identification of invasion specific splice variants of the cytoskeletal protein Mena present in mammary tumor cells during invasion in vivo. Clin Exp Metastasis. 2009; 26:153–9. [PubMed: 18985426]
23. Roussos ET, Balsamo M, Alford SK, Wyckoff JB, Gligorijevic B, Wang Y, et al. Mena invasive (MenaINV) promotes multicellular streaming motility and transendothelial migration in a mouse model of breast cancer. J Cell Sci. 2011; 124:2120–31. [PubMed: 21670198]
24. Agarwal S, Gertler FB, Balsamo M, Condeelis JS, Camp RL, Xue X, et al. Quantitative assessment of invasive mena isoforms (Menacalc) as an independent prognostic marker in breast cancer. Breast Cancer Res. 2012; 14:R124. [PubMed: 22971274]
25. Forse CL, Agarwal S, Pinnaduwage D, Gertler F, Condeelis JS, Lin J, et al. Menacalc, a quantitative method of metastasis assessment, as a prognostic marker for axillary node-negative breast cancer. BMC Cancer. 2015; 15:483. [PubMed: 26112005]
26. Oudin, MJ., Hughes, SK., Rohani, N., Moufarrej, MN., Jones, JG., Condeelis, JS., et al. Characterization of the expression of the pro-metastatic Mena(INV) isoform during breast tumor progression. Clin Exp Metastasis. 2015. Available from: http://www.ncbi.nlm.nih.gov/pubmed/26680363
27. Philippar U, Roussos ET, Oser M, Yamaguchi H, Kim H-D, Giampieri S, et al. A Mena Invasion Isoform Potentiates EGF-Induced Carcinoma Cell Invasion and Metastasis. Dev Cell. 2008; 15:813–28A. [PubMed: 19081071]
28. Hughes, SK., Oudin, MJ., Tadros, J., Neil, J., Del Rosario, A., Joughin, BA., et al. PTP1B-dependent regulation of receptor tyrosine kinase signaling by the actin-binding protein Mena. Mol Biol Cell. 2015. Available from: http://www.ncbi.nlm.nih.gov/pubmed/26337385
29. Anders CK, Zagar TM, Carey LA. The management of early-stage and metastatic triple-negative breast cancer: a review. Hematol Oncol Clin North Am. 2013; 27:737–49. viii. [PubMed: 23915742]
30. Gertler FB, Niebuhr K, Reinhard M, Wehland J, Soriano P. Mena, a relative of VASP and Drosophila enabled, is implicated in the control of microfilament dynamics. Cell. 1996; 87:227–39. [PubMed: 8861907]
31. Laughney AM, Kim E, Sprachman MM, Miller MA, Kohler RH, Yang KS, et al. Single-cell pharmacokinetic imaging reveals a therapeutic strategy to overcome drug resistance to the microtubule inhibitor eribulin. 2014:6.
32. Gupton SL, Riquelme D, Hughes-Alford SK, Tadros J, Rudina SS, Hynes RO, et al. Mena binds α5 integrin directly and modulates α5β1 function. J Cell Biol. 2012; 198:657–76. [PubMed: 22908313]
33. Lebrand C, Dent EW, Strasser GA, Lanier LM, Krause M, Svitkina TM, et al. Critical role of Ena/VASP proteins for filopodia formation in neurons and in function downstream of netrin-1. Neuron. 2004; 42:37–49. [PubMed: 15066263]

34. Comprehensive molecular portraits of human breast tumours. Nature. 2012; 490:61–70. [PubMed: 23000897]
35. Wang L, Zhao Z, Meyer M, Saha S, Yu M, Guo A, et al. CARM1 methylates chromatin remodeling factor BAF155 to enhance tumor progression and metastasis. Cancer Cell. 2014; 25:21–36. [PubMed: 24434208]
36. Mcgrail DJ, Khambhati NN, Qi MX, Patel KS, Ravikumar N. Alterations in Ovarian Cancer Cell Adhesion Drive Taxol Resistance by Increasing Microtubule Dynamics in a FAK-dependent Manner. Sci Rep. 2015; 5:9529. [PubMed: 25886093]
37. Song Y, Brady ST. Post-translational modifications of tubulin: pathways to functional diversity of microtubules. Trends Cell Biol. 2015; 25:125–36. [PubMed: 25468068]
38. Trono P, Di Modugno F, Circo R, Spada S, Di Benedetto A, Melchionna R, et al. hMENA11a contributes to HER3-mediated resistance to PI3K inhibitors in HER2-overexpressing breast cancer cells. Oncogene. 2016; 35:887–96. [PubMed: 25961924]
39. Stehbens S, Wittmann T. Targeting and transport: how microtubules control focal adhesion dynamics. J Cell Biol. 2012; 198:481–9. [PubMed: 22908306]
40. Chesarone MA, DuPage AG, Goode BL. Unleashing formins to remodel the actin and microtubule cytoskeletons. Nat Rev Mol Cell Biol. 2010; 11:62–74. [PubMed: 19997130]
41. Bartolini F, Andres-Delgado L, Qu X, Nik S, Ramalingam N, Kremer L, et al. An mDia1-INF2 formin activation cascade facilitated by IQGAP1 regulates stable microtubules in migrating cells. Mol Biol Cell. 2016; 27:1797–808. [PubMed: 27030671]
42. Henty-Ridilla JL, Rankova A, Eskin JA, Kenny K, Goode BL. Accelerated actin filament polymerization from microtubule plus ends. Science. 2016; 352:1004–9. [PubMed: 27199431]
43. Long JB, Bagonis M, Lowery LA, Lee H, Danuser G, Van Vactor D. Multiparametric analysis of CLASP-interacting protein functions during interphase microtubule dynamics. Mol Cell Biol. 2013; 33:1528–45. [PubMed: 23382075]
44. Schmid-Alliana A, Menou L, Manié S, Schmid-Antomarchi H, Millet MA, Giuriato S, et al. Microtubule integrity regulates src-like and extracellular signal-regulated kinase activities in human pro-monocytic cells. Importance for interleukin-1 production. J Biol Chem. 1998; 273:3394–400. [PubMed: 9452460]
45. Shinohara-Gotoh Y, Nishida E, Hoshi M, Sakai H. Activation of microtubule-associated protein kinase by microtubule disruption in quiescent rat 3Y1 cells. Exp Cell Res. 1991; 193:161–6. [PubMed: 1847331]
46. Di Modugno F, Mottolese M, DeMonte L, Trono P, Balsamo M, Conidi A, et al. The cooperation between hMena overexpression and HER2 signalling in breast cancer. PLoS One. 2010; 5:e15852. [PubMed: 21209853]
47. Aoudjit F, Vuori K. Integrin signaling inhibits paclitaxel-induced apoptosis in breast cancer cells. Oncogene. 2001; 20:4995–5004. [PubMed: 11526484]
48. McDaid HM, Lopez-Barcons L, Grossman A, Lia M, Keller S, Pérez-Soler R, et al. Enhancement of the therapeutic efficacy of taxol by the mitogen-activated protein kinase kinase inhibitor CI-1040 in nude mice bearing human heterotransplants. Cancer Res. 2005; 65:2854–60. [PubMed: 15805287]
49. Yacoub A, Han SI, Caron R, Gilfor D, Mooberry S, Grant S, et al. Sequence dependent exposure of mammary carcinoma cells to Taxotere and the MEK1/2 inhibitor U0126 causes enhanced cell killing in vitro. Cancer Biol Ther. 2:670–6.
50. MacKeigan JP, Collins TS, Ting JP. MEK inhibition enhances paclitaxel-induced tumor apoptosis. J Biol Chem. 2000; 275:38953–6. [PubMed: 11038347]
51. Coupe N, Corrie P, Hategan M, Larkin J, Gore M, Gupta A, et al. PACMEL: a phase 1 dose escalation trial of trametinib (GSK1120212) in combination with paclitaxel. Eur J Cancer. 2015; 51:359–66. [PubMed: 25542057]
52. Mamounas EP, Bryant J, Lembersky B, Fehrenbacher L, Sedlacek SM, Fisher B, et al. Paclitaxel After Doxorubicin Plus Cyclophosphamide As Adjuvant Chemotherapy for Node-Positive Breast Cancer: Results From NSABP B-28. J Clin Oncol. 2005; 23:3686, 3696. [PubMed: 15897552]
53. Noguchi S. Predictive factors for response to docetaxel in human breast cancers. Cancer Sci. 2006; 97:813–20. [PubMed: 16805818]

54. Rohan TE, Xue X, Lin H-M, D'Alfonso TM, Ginter PS, Oktay MH, et al. Tumor microenvironment of metastasis and risk of distant metastasis of breast cancer. J Natl Cancer Inst. 2014:106.

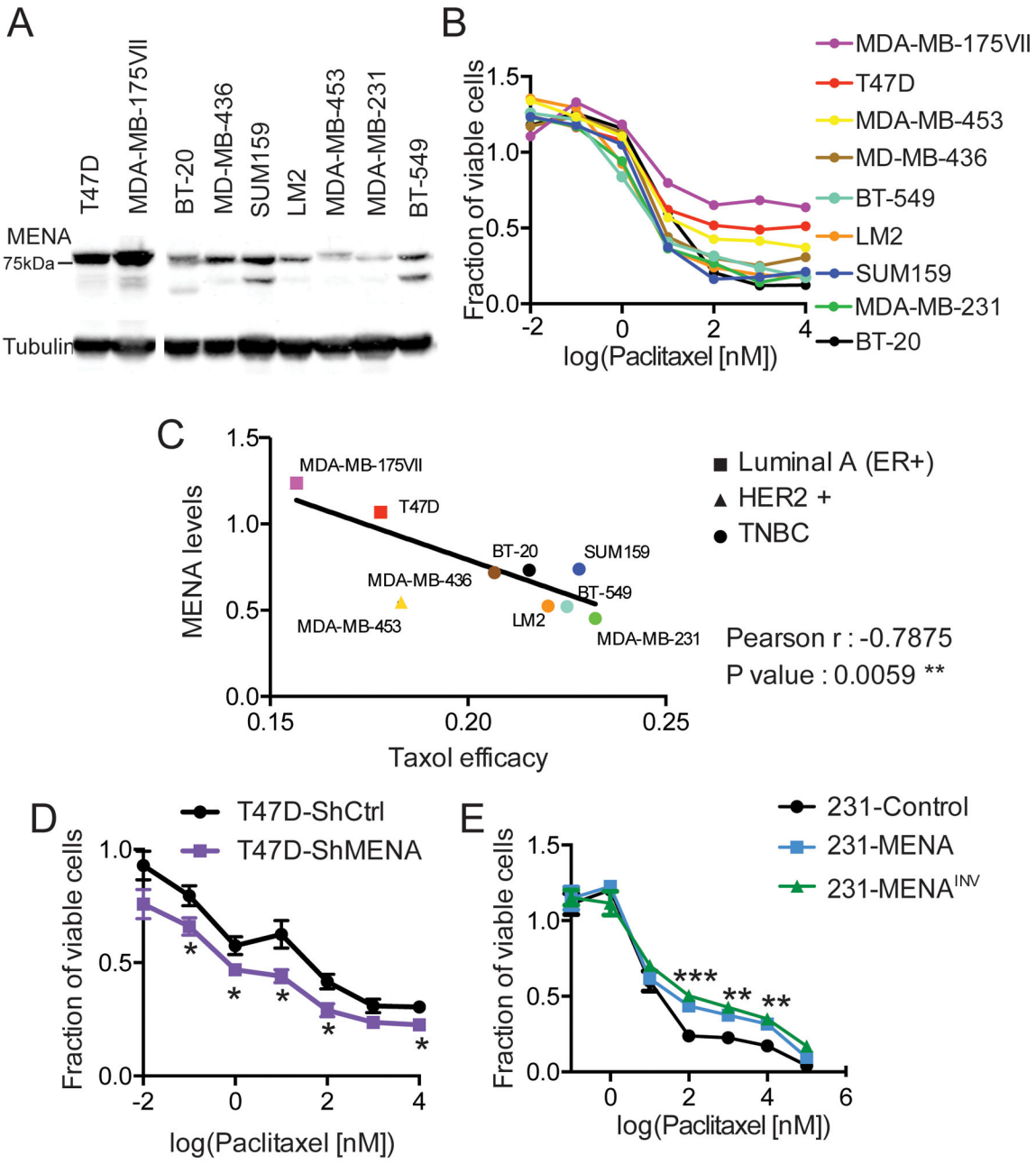

Figure 1. Expression of MENA isoforms is associated with paclitaxel resistance

(A) Representative western blot of lysate prepared from the panel of breast cancer cell lines MDA-MB 175IIV and T47D (Luminal A, square), MDA-MB 453 (HER2+, triangle), MDA-MB 436, BT-549, LM2, SUM159, MDA-MB 231 and BT-20 (TNBC, circle), probed with anti-MENA and anti-Tubulin antibodies (n=3). MENA expression level was assessed by measuring intensity of 80kDa band. (B) Cell viability at 72h was assessed for the same cell lines as in *A*, showing mean dose response across n=3. (C) Linear correlation between MENA protein expression (*A*) and paclitaxel efficacy, here defined as the inverse of the area under the dose response in *B* (n=3). (D) Cell viability in T47D cells expressing ShCtrl or

ShMENA after 72h of treatment with paclitaxel, determined using Prestoblue assay. (E) Cell viability was assessed in 231-Control, 231-MENA or 231-MENA^{INV} cells after 72h of treatment with paclitaxel, determined using Prestoblue assay. The cell viability is expressed as a fraction relative to untreated cells. Data presented as mean± SEM for three independent experiments, each performed in duplicate. Statistics determined by unpaired t-test with Welch's correction, where *** $p<0.001$, ** $p<0.01$, * $p<0.05$.

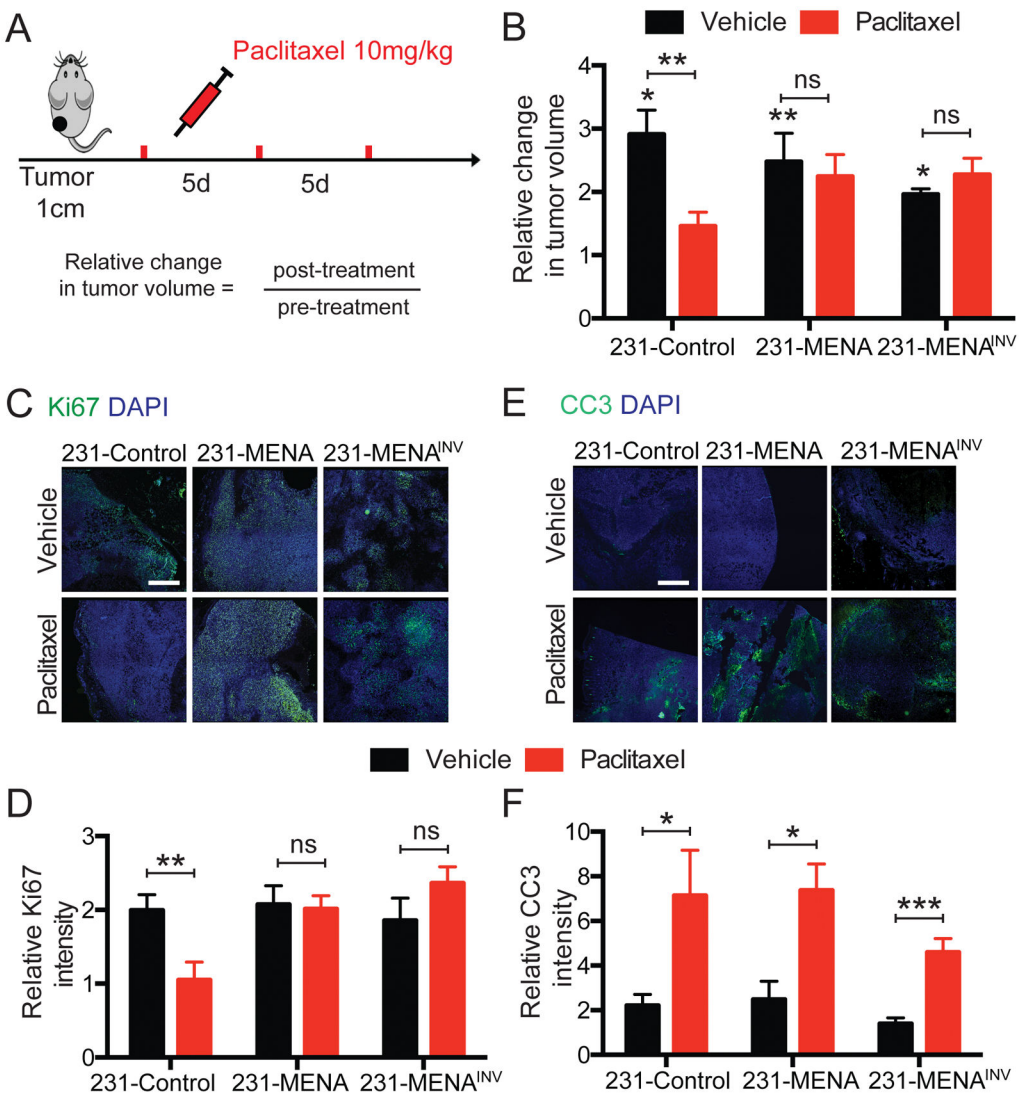

Figure 2. MENA or MENA^{INV} expression weakened paclitaxel effect on tumor growth *in vivo*

(A) Tumors were generated by injection of 231-Control, 231-MENA or 231-MENA^{INV} cells in the mammary fat pad of NOD SCID mice. When tumors reached 1cm in diameter, mice were treated with paclitaxel every 5 days, 3 doses at 10mg/kg IP. Tumor volume was measured before and after treatment. (B) Relative change in tumor volume after treatment with paclitaxel of tumors expressing the different GFP-tagged MENA isoforms. Data presented as mean± SEM for at least 9 mice in each group. Statistics determined by unpaired t-test, where *** $p<0.001$, ** $p<0.01$, * $p<0.05$. (C) Representative images tumor sections from 231-Control, MENA and MENA^{INV}, treated with vehicle or paclitaxel, and stained for the proliferation marker Ki67 (green). Scale bar is 100μm. (D) Quantification of the Ki67 staining intensity in 231-Control, MENA and MENA^{INV} tumors, with and without paclitaxel treatment. (E) Representative images tumor sections from 231-Control, MENA and MENA^{INV}, treated with vehicle or paclitaxel, and stained for the apoptosis marker Cleaved-Caspase 3 (CC3) (green). Scale bar is 100μm. (F) Quantification of the CC3 staining intensity in 231-Control, MENA and MENA^{INV} tumors, with and without paclitaxel

treatment. Data presented as mean± SEM for at 3 mice in each group, with at least 5 fields of view per tumor. Statistics determined by unpaired t-test, where *** $p<0.001$, ** $p<0.01$, * $p<0.05$.

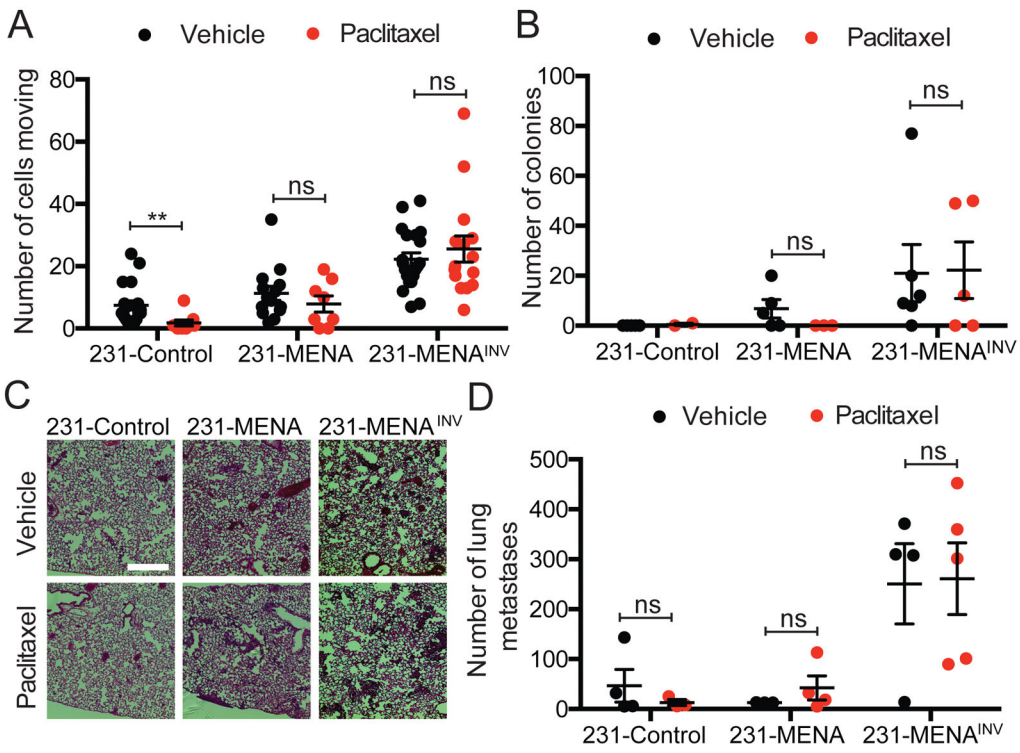

Figure 3. Paclitaxel treatment does not affect MENA^{INV}-driven tumor cell motility and dissemination in mice

(A) Quantification of motile cells by multiphoton intravital imaging in tumors expressing MENA, MENA^{INV} or Control. Tumors grown in mice treated with paclitaxel or vehicle. Data presented as mean± SEM, pooled from at least 3 mice per condition, with at least 2 fields of view per mouse. (B) Number of disseminated tumor cells corresponding to the number of colonies in cultured bone marrow collected from mice bearing 231-Control, 231-MENA or 231-MENA^{INV} tumors, 12 weeks after injection. (C) Representative images of H&E stained lungs from mice bearing Control, 231-MENA or 231-MENA^{INV} tumors, treated with vehicle or paclitaxel. Scale bar is 100μm. (D) Number of metastases in lung of mice bearing Control, 231-MENA or 231-MENA^{INV} tumors 12 weeks after injection. Data presented as mean± SEM for at least 3 mice per group. Statistics determined by unpaired t-test, where *** $p<0.001$, ** $p<0.01$, * $p<0.05$.

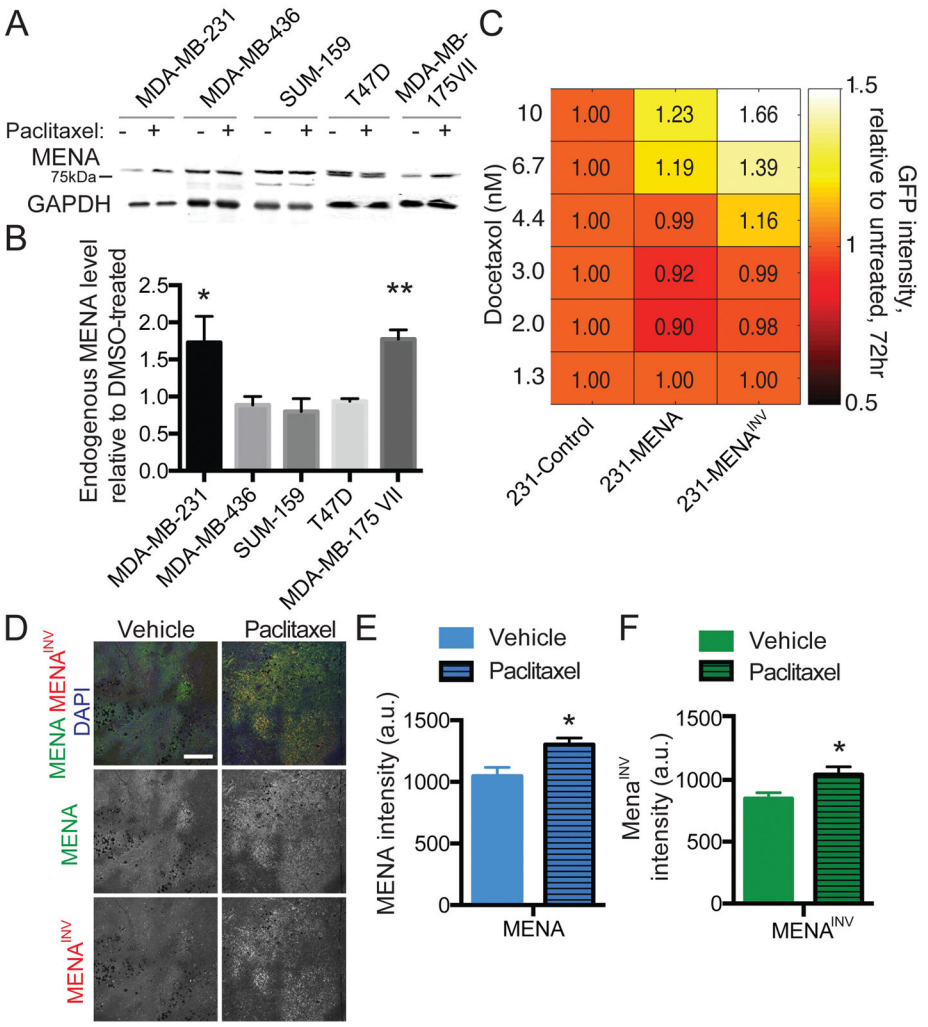

Figure 4. Paclitaxel treatment selects for high MENA expression *in vitro* and *in vivo*

(A) Representative western blot of whole cell lysates prepared from multiple breast cancer cell lines treated with 100nM paclitaxel or DMSO as vehicle for 72 hours and probed with anti-MENA and anti-GAPDH antibodies. Images are not all from the same blots. (B) Quantification of endogenous MENA levels after 100nM paclitaxel relative to DMSO-treated. Data presented as mean± SEM for three independent experiments. (C) FACS analysis of GFP expression levels of 231-Control, 231-MENA and 231-MENA^{INV} cells treated with Docetaxol for 72hrs. The number shows the fold change in GFP signal relative to 231-Control cells. (D) Representative images of FFPE section from 231-Control tumor grown in mice treated with paclitaxel or with vehicle and stained for MENA (green), MENA^{INV} (red) and DAPI (blue). Scale bar = 200μm. Mean of MENA (E) and MENA^{INV} (F) fluorescence signal intensity. Data presented as mean± SEM for 10 fields of view per tumor, from 3 different mice. Statistics determined by unpaired t-test, where * $p<0.05$.

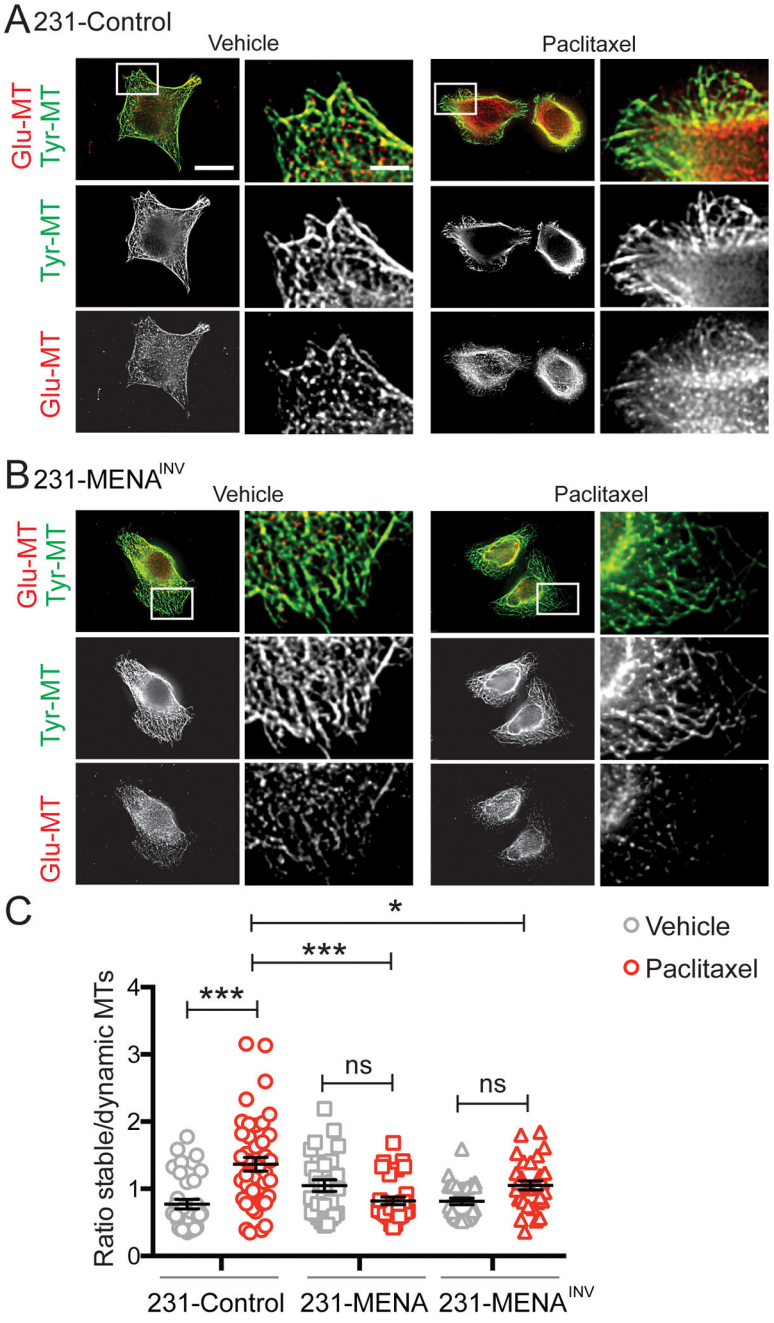

Figure 5. MENA expression alters MT dynamics during paclitaxel treatment

Representative images of 231-Control (A) and 231-MENA^{INV} (B) cells treated with paclitaxel (10nM) for 24h, and immunostained for detyrosinated or Glu-Tubulin (red) and tyrosinated or Tyr-Tubulin (green). Scale bar is 1 μm, and 0.25 μm in inset. (C) Quantification of the ratio of Glu-MT relative to Tyr-MT in 231-Control, MENA or MENA^{INV} cells treated with vehicle (0.01% DMSO) or 10nM paclitaxel for 24h. Data presented as mean± SEM. Data pooled from 3 separate experiments, at least 8 cells analyzed per experiment. Statistics determined by one-way ANOVA, where *** p<0.001, ** p<0.01, * p<0.05.

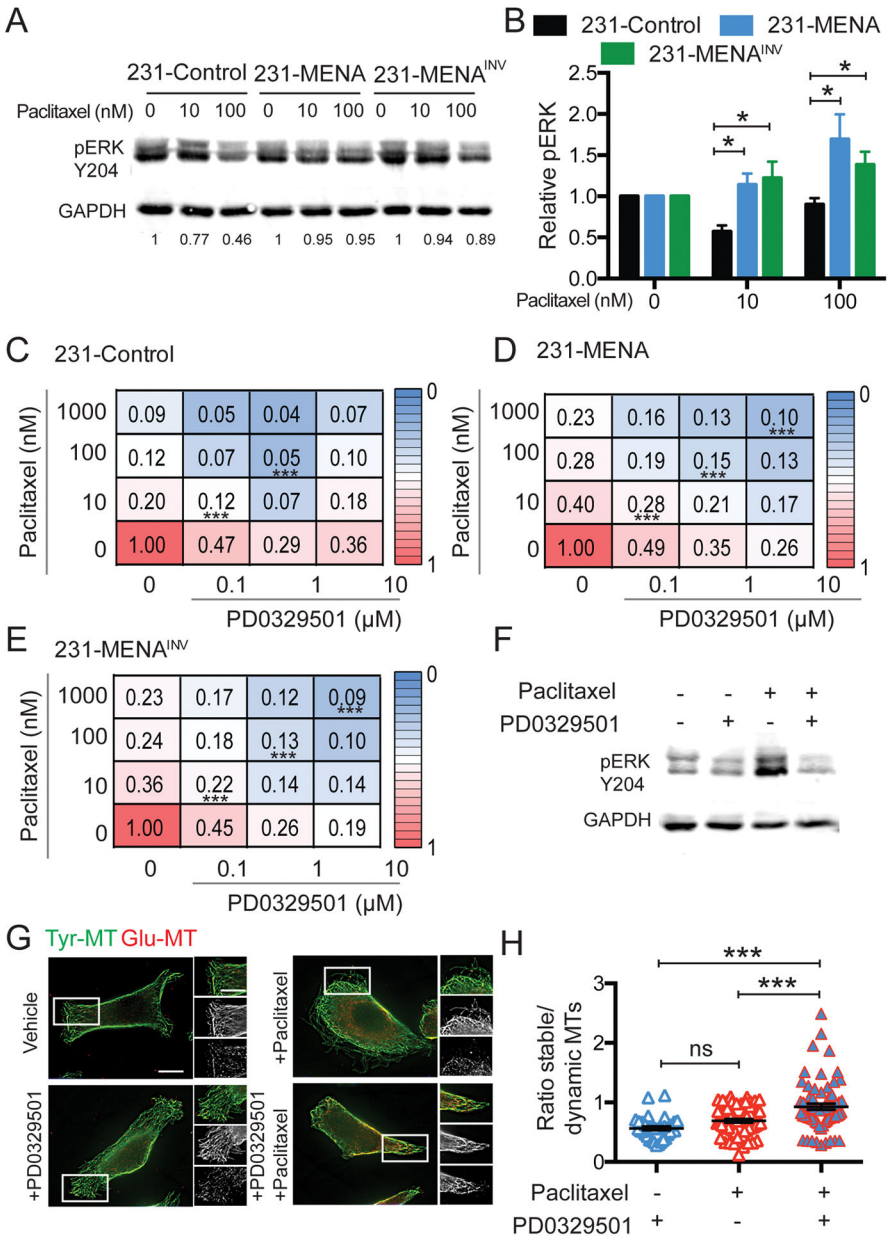

Fig 6. MENA isoforms confer resistance to paclitaxel by increasing MAPK signaling

(A) Representative Western Blot for pERK Y204 for in 231-Control, MENA or MENA^{INV} cells treated with vehicle (0.01% DMSO), 10 or 100nM paclitaxel for 72h. Loading control is GAPDH. (B) Quantification of Western Blot shown in A, for pERK relative to GAPH. Data pooled from 4 experiments, two technical replicates per experiment. 231-Control (C), 231-MENA (D) and 231-MENA^{INV} (E) cells were treated with varying combinations of MEKi PD0329501 and paclitaxel for 72h, after which cell count was measured (shown as numbers and heatmap as a fraction of the max cell count for each plate). (F) Representative Western Blot for pERK Y204 for 231-MENA^{INV} cells treated with vehicle (0.01% DMSO), 10nM paclitaxel, 0.1 μM PD0329501 alone or in combination for 72h. Loading control is GAPDH. (G) Representative images 231-MENA^{INV} cells with vehicle (0.01% DMSO),

10nM paclitaxel, 0.1 μM PD0329501 alone or in combination for 24h, and immunostained for detyrosinated or Glu-Tubulin (red) and tyrosinated or Tyr-Tubulin (green). Scale bar is 1μm, 0.25 μm in inset. (H) Quantification of the ratio of Glu-MT relative to Tyr-MT in 231-MENA^{INV} cells treated with vehicle (0.01% DMSO) or 10nM paclitaxel for 24h. Data pooled from 3 separate experiments, at least 8 cells analyzed per experiment. Data presented as mean± SEM. Statistics determined by one-way ANOVA, where *** $p<0.001$, ** $p<0.01$, * $p<0.05$.